ORGANIC LETTERS

2002
Vol. 4, No. 20
3367−3370

Regioselective Synthesis of Antiparallel Loops on a Macrocyclic Scaffold Constrained by Oxazoles and Thiazoles

Yogendra Singh, Martin J. Stoermer, Andrew J. Lucke, Matthew P. Glenn, and David P. Fairlie*

Centre for Drug Design and Development, Institute for Molecular Bioscience, University of Queensland, Brisbane, Qld 4072, Australia

d.fairlie@imb.uq.edu.au

Received July 3, 2002

ABSTRACT

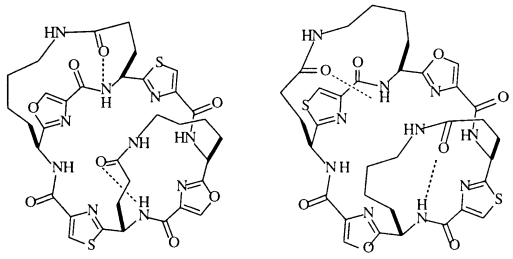

3 **7**

The regioselective syntheses and structures are reported for two tris-macrocylic compounds, each possessing two antiparallel loops on a macrocyclic scaffold constrained by two oxazoles and two thiazoles. NMR solution structures show the loops projecting from the same face of the macrocycle. Such molecules are shown to be prototypes for mimicking multiple loops of proteins.

Protein loops are common recognition motifs in biology, yet creation of small molecules to structurally mimic bioactive, multiloop surfaces remains a challenging objective.[1,2] We were inspired by Nature's use in bacteria, fungi, plants, and marine organisms of unusual amino acids containing oxazoles/thiazoles and their reduced analogues as constraints to regulate the shapes[3] of macrocycles[4] like ascidiacyclamide **1**,[4b] nostocyclamide,[4c] and thiopeptide antibiotics.[4d] Related cyclic peptides show antitumor, antiinflammatory, immunoregulating, and enzyme-inhibiting activities.[5] In ulithiacyclamide **2**,[4e] the macrocycle is a scaffold supporting one disulfide bridge. Here we report an efficient regioselective synthesis and solution structure of tris-macrocycle **3**, with

(1) (a) Fairlie, D. P.; West, M. L.; Wong, A. K *Curr. Med. Chem.* **1998**, *5*, 29−62. (b) Reineke, U.; Schneider-Mergener, J. *Angew. Chem., Int. Ed.* **1998**, *37*, 769−771.

(2) (a) Bisang, C.; Weber, C.; Robinson, H. A. *Helv. Chim. Acta* **1996**, *79*, 1825−1841. (b) Mutter, M.; Dumy, P.; Garrouste, P.; Lehmann, C.; Mathieu, M.; Peggion, C.; Peluso, S.; Razaname, A.; Tuchscherer, G. *Agnew. Chem., Int. Ed. Engl.* **1996**, *35*, 1482−1485. (c) Hamuro, Y.; Calama, M. C.; Park, H. S.; Hamilton, A. D. *Agnew. Chem., Int. Ed. Engl.* **1997**, *36*, 2680−2683. (d) Favre, M.; Moehle, K.; Jiang, L.; Pfeiffer, B.; Robinson, J. A. *J. Am. Chem. Soc.* **1999**, *121*, 2679−2685.

(3) (a) Fairlie, D. P.; Abbenante, G.; March, D. R. *Curr. Med. Chem.* **1995**, *2*, 654−86. (b) Abbenante, G.; Fairlie, D. P.; Gahan, L. R.; Hanson, G. R.; Pierens, G.; van den Brenk, A. L. *J. Am. Chem. Soc.* **1996**, *118*, 10384−10388.

(4) (a) Wipf, P. *Chem. Rev.* **1995**, *95*, 2115−2134. (b) Ishida, T.; Inoue, M.; Hamada, Y.; Kato, S.; Shiori, T. *J. Chem. Soc., Chem. Commun.* **1987**, 370−371. (c) Todorova, A. K.; Juttner, F.; Linden, A.; Pluss, T.; von Philipsborn. W. *J. Org. Chem.* **1995**, *60*, 7891−7895. (d) Toske, S. G.; Fenical, W. *Tetrahedron Lett.* **1995**, *36*, 8355−8. (e) Ireland, C. M.; Scheuer, P. J. *J. Am. Chem. Soc.* **1980**, *102*, 5688−5691. (f) Sowinski, J.; Toogood, P. L. *Tetrahedron Lett.* **1995**, *36*, 67−70. (g) Fate, G. D.; Benner, C. P.; Grode, S. H.; Gilbertson, T. J. *J. Am. Chem. Soc.* **1996**, *118*, 11363−11368. (h) McGeary, R. P.; Fairlie, D. P. *Curr. Opin. Drug Discuss. Dev.* **1998**, *1*, 208−217.

(5) (a) Mocek, U.; Zeng, Z.; O'Hagan, D.; Zhou, P.; Fan, L.-D. G.; Beale, J. M.; Floss, H. G. *J. Am. Chem. Soc.* **1993**, *115*, 7992−8001. (b) Rinehart, J. B.; Gloer, J. B.; Cock, J. C.; Mizsak, S. A.; Scahill, T. A. *J. Am. Chem. Soc.* **1981**, *103*, 1857. (c) Rinehart, K. L.; Kishure, V.; Bible, K. C.; Sakai, R.; Sullins, D. W.; Li, K. M. *J. Nat. Prod.* **1988**, *51*, 1−21. (d) Ireland, C. M.; Durso, A. R.; Newman, R. A.; Hacker, M. P. *J. Org. Chem.* **1982**, *47*, 1807−1811. (e) Shioiri, T.; Hamada, Y.; Kato, S.; Shibata, M.; Kondo, Y.; Nakagawa, H.; Kohda, K. *Biochem. Pharm.* **1987**, *36*, 4181−4185.

10.1021/ol026463m CCC: $22.00
Published on Web 09/11/2002

two antiparallel loops containing oxazole projecting perpendicularly from the same face of a macrocyclic scaffold **6** constrained by oxazoles and thiazoles. The alternative tris-macrocycle isomer **7**, in which the loops contain thiazole instead of oxazole, was independently synthesized and structurally characterized by NMR spectroscopy. Molecular models suggest that scaffold **6** could be suitable for mimicking multiloop surfaces of proteins such as interhelical loops from helix bundles and complementarity-determining loops of antibodies.

Functionalized dipeptide surrogates Boc-L-Lys(Cbz)(Ox)-OH (**4a** X = O, R = $-(CH_2)_4NHCO_2Bn$)[6] and L-Glu(OcHx)-(Thz)-OH (**4b**, X = S, R = $-(CH_2)_2CO_2cHx$)[7a] were elaborated to tetrapeptide analogue **5** ($R_1 = -(CH_2)_4NHCO_2Bn$, $R_2 = -(CH_2)_2CO_2cHx$). Cyclodimerization of **5** (Scheme 1) followed by deprotection gave a high isolated yield (84%)

Scheme 1[a]

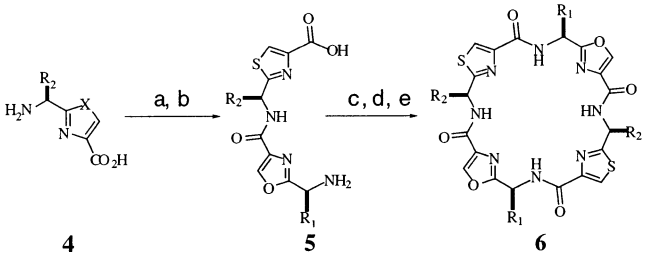

[a] Reaction conditions: (a) BOP, DIPEA, DMF, **4b**, rt (97%). (b) TFA, CH2 Cl_2, ~0 °C (100%). (c) BOP, DIPEA, DMF (7×10^{-3} M), rt. (d) $NaHCO_3$. (e) HF, *p*-cresol (84% from **5**).

of cyclic octapeptide analogue **6** ($R_1 = -(CH_2)_4NH_2$, $R_2 = -(CH_2)_2CO_2H$).[8] Dimerization is favored over cyclooligomerization[7b] (~16%) by the presence of two turn-inducing heterocyclic oxazole/thiazole constraints. NMR spectra (^1H, ^{13}C) for **6** indicate C_2 fold symmetry.

Molecular modeling[9] (Figure 2) identified **6** as a rigid, rhombus-shaped macrocycle (~6.5 × ~6.6 Å) similar to the marine natural product ascidiacyclamide (**1**).[4b] It has a C_2 fold axis of symmetry with the two thiazoles tilted ~90° out of the macrocycle plane. The flexible L-Lys and L-Glu side

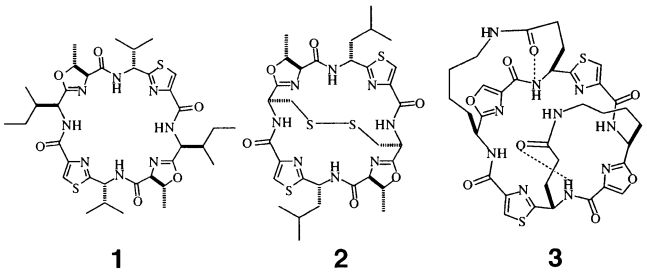

Figure 1. Natural products **1** and **2** and synthetic target **3**.

chains are directed from the same face of the macrocycle, as in other oxazole- or thiazole-containing macrocycles,[10] suggesting **6** as a likely scaffold for supporting discontinuous loops.

As a prelude to grafting loops from protein surfaces onto scaffold **6**, we prepared prototypes **3** and **7** (isolated yields: 71 and 1%, respectively)[11] by coupling L-Lys and L-Glu side chains of **6** (Scheme 2).

Compound **3** was highly symmetrical, displaying one set of ^1H and ^{13}C resonances, indicative of C_2 fold symmetry. The chemical shifts for Lys αNH (δ 8.33, $^3J_{NH-\alpha H} = 9.06$ Hz) and Lys ϵNH (δ 7.73) resonances of **3** in DMSO-d_6 are temperature dependent ($\Delta\delta/T$ 4.9, 3.6 ppb/K, respectively) and exchange rapidly upon addition of 5% D_2O. By contrast, the Glu αNH resonance (δ 8.22, $^3J_{NH-\alpha H} = 7.96$ Hz) for **3** is almost temperature independent ($\Delta\delta/T$ 0.46 ppb/K) and only exchanges slowly with D_2O, features consistent with a hydrogen bond, the H-bond acceptor being identified as the Glu-γ-CO by ROEs (see below). The different $^3J_{NH-\alpha H}$ values for Glu and Lys amide-NHs of the scaffold translate, via the Karplus equation, to NHαCH dihedral angles of 148 and 158°, respectively, which in turn correspond to Φ angles of −150 (Glu) and −140° (Lys). The conformational strain in **3** is evidenced by significant chemical shift differences for several pairs of geminal protons within the loop portion of the molecule (Glu βHs 0.54, Glu γHs 0.23, Lys βHs 0.83, Lys ϵHs 1.13 ppm), consistent with their differing orientations above the macrocyclic template.

ROE data support the presence of a H-bond between Glu NH···OCγ Glu, with correlations between Glu γH (δ 2.16)

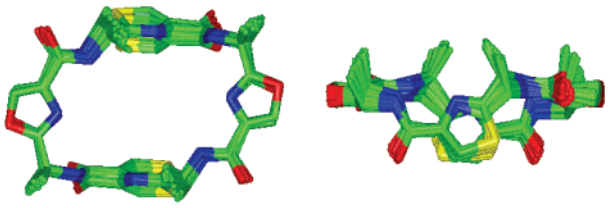

Figure 2. Superposition of 59 low energy conformations of **6** (ΔE < 11.5 kJ/mol, RMSD < 0.7 Å for 24 atoms) viewed top down (left) and side on (right); side chains are omitted for clarity.

(6) The oxazole was prepared from Boc-Lys(Z)Ser-OMe by cyclodehydration (DAST) followed by oxidation ($BrCCl_3$/DBU): Phillips, A. J.; Uto, Y.; Wipf, P.; Reno, M. J.; Williams, D. R. *Org. Lett.* **2000**, *2*, 1165−1168.

(7) (a) Singh, Y.; Sokolenko, N.; Kelso, M. J.; Gahan, L. R.; Abbenante, G.; Fairlie, D. P. *J. Am. Chem. Soc.* **2001**, *123*, 333−334. (b) Sokolenko, N.; Abbenante, G.; Scanlon, M. J.; Jones, A.; Gahan, L. R.; Hanson, G. R.; Fairlie, D. P. *J. Am. Chem. Soc.* **1999**, *121*, 2603−2604.

(8) TFA·H-Lys(Z)(Ox)Glu(OcHx)(Thz)-OH (**5**, 1.4 g, 1.9 mmol) and BOP (1.1 g, 2.5 mmol) were dissolved in DMF (260 mL) and stirred with DIPEA (1.1 mL, 6.3 mmol) at 20 °C for 24 h. Workup, HF cleavage, and HPLC purification yielded **6** (812 mg, 84%; HRMS: (M + H) found 815.2599, calcd 815.2605).

(9) (a) MacroModel: Mohamadi, F.; Richards, N. G. J.; Guida, W. C.; Kiskamp, R.; Lipton, M.; Caufield, C.; Chang, G.; Hendrickson, T.; Still, W. C. *J. Comput. Chem.* **1990**, *112*, 440−447. (b) Monte Carlo (MCMM): Chang, G.; Guida, W. C.; Still, W. C. *J. Am. Chem. Soc.* **1989**, *111*, 4379−4386. (c) Search, AMBER*: McDonald, D. Q.; Still, W. C. *Tetrahedron Lett.* **1992**, *33*, 7743−7746. (d) Force field, water GB/SA solvent continuum: Still, W. C.; Tempczyk, A.; Hawely, R. C.; Hendrickson, T. *J. Am. Chem. Soc.* **1990**, *112*, 6127−6129. (e) Minimization: Polak, E.; Ribiere, G. *Rev. Fr. Inf. Rech. Oper.* **1969**, 16−R1, 35.

Scheme 2. Cyclization of **6**·2TFA (1×10^{-3} M) from 0 to 20 °C gives a 10:1 ratio of **3** and **7**.[11]

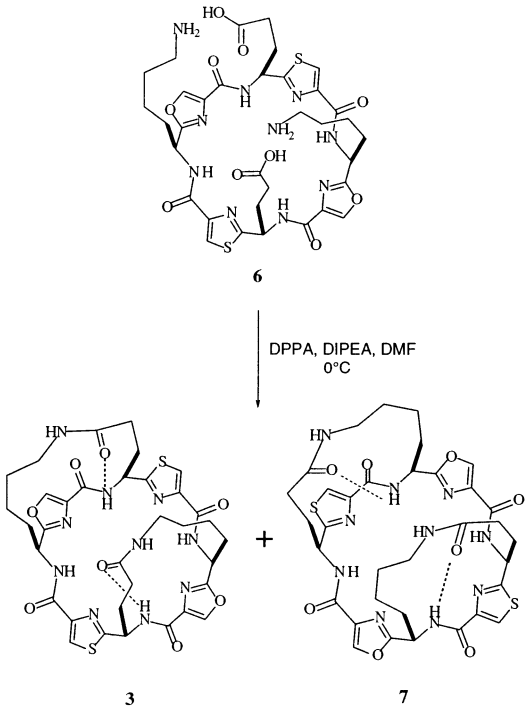

Scheme 3[a]

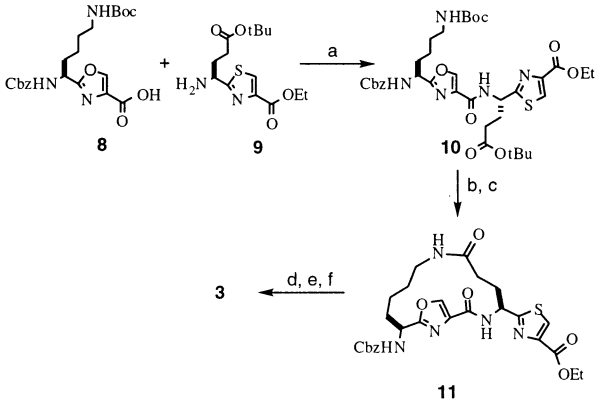

[a] Reaction conditions: (a) BOP, DIPEA, DMF, rt (98%). (b) TFA, CH_2Cl_2, ~0 °C (100%). (c) BOP, DIPEA, DMF (6×10^{-3} M), rt (91%). (d) LiOH, EtOH/H_2O (3:1), ~0 °C. (e) HF, *p*-cresol (90% from **10**). (f) BOP, DIPEA, DMF (6×10^{-3} M), rt (78%).

and Glu NH (medium) and between Glu NH and Lys ϵNH (weak). The latter indicates that the loops incorporate oxazole rather than thiazole. Other intraloop correlations between Lys αNH and Lys δH (δ1.44, weak; 1.14, strong) and Lys βH (δ 2.54) and Lys ϵH (δ 3.86, strong) as well as interloop correlations between Glu αNH and Lys βH (δ 2.54, vs weak) and Glu αNH and Lys γH (δ 1.14, vs weak) define the locations of the two loops.

The identity of the loops was confirmed by an alternative independent synthesis of **3** (Scheme 3) by coupling Cbz-L-Lys(Boc)(Ox)-OH **8** to L-Glu(OtBu)(Thz)-OEt **9** to give Cbz-Lys(Boc)(Ox)Glu(OtBu)(Thz)OEt **10**. Subsequent loop formation to **11** preceded dimerization to **3**.

After modification of standard topology and parameter files (Supporting Information) to accommodate the unnatural dipeptide surrogates, the structure of **3** was calculated in XPLOR[12] using only the two Lys dihedral angle restraints ($F = -120 \pm 30°$). The resulting convergent structures were refined using 60 ROE distance constraints and the two H-bonds described above. The 20 lowest energy ($E < 10$ kJ/mol) calculated structures, shown superimposed in Figure 3, had no residual distance (>0.16 Å), H-bond, or dihedral angle violations. There was tight convergence of the macrocyclic scaffold (RMSD 0.2 Å), while the loops retained some flexibility (RMSD 1.8 Å).

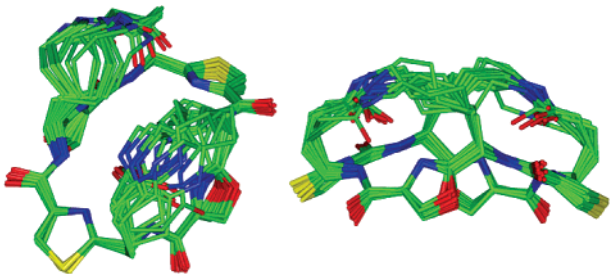

Figure 3. Superimposition of the 20 lowest energy NMR structures of **3** shown top down (left) and side on (right).

The thiazole-containing macrocyclic component of **3** differs from the modeled template **6** in that the oxazoles are now (90° out of the plane of the thiazole-containing macrocycle and in the plane of the oxazole-containing loops. The thiazoles are tilted 20−30° (instead of 90°) down from the plane of the macrocycle corresponding to **6**. The Cα−Cβ vectors are 6 Å apart and project from the same face of the scaffold, directing both oxazole−containing loops perpendicularly and staggered relative to one another.

(10) (a) Mink, D.; Mecozzi, S.; Rebek, J., Jr. *Tetrahedron Lett.* **1998**, *39*, 5709−5712. (b) Haberhauer, G.; Somogyi, L.; Rebek, J., Jr. *Tetrahedron Lett.* **2000**, *41*, 5013−5016. (c) Somogyi, L.; Haberhauer, G.; Rebek, J., Jr. *Tetrahedron Lett.* **2001**, *57*, 1699−1708. (d) Boss, C.; Rasmussen, P. H.; Wartini, A. R.; Waldvogel, S. R. *Tetrahedron Lett.* **2000**, *41*, 6327−6331. (e) Bertram, A.; Hannam, J. S.; Jolliffe, K. A.; Gonzalez-Lopez de Turiso, F.; Pattenden, G. *Synlett* **1999**, *11*, 1723−1726.

(11) DIPEA (0.2 mL, 1.15 mmol) was added to **6**·2TFA (90 mg, 0.085 mmol) and DPPA (60 μL, 2.78 mmol) in dry DMF (70 mL) at 0 °C and stirred (2 h, 0 °C.; 48 h, 20 °C), concentrated, and purified by rpHPLC to give **3** (48 mg, 71%; HRMS: (M + H) found 779.2388, calcd 779.2392) and side product **7** (1% yield). Both **3** and **7** were subsequently synthesized independently (**1f-1t**, Supporting Information). When BOP was used for coupling, hydroxybenzotriazole was trapped by **3**, coeluting from rpHPLC columns and detectable in ^{1}H NMR spectra.

(12) XPLOR 3.851 using a dynamic simulated annealing protocol in a geometric force field and minimized using CHARm: (a) Brünger, A. T. *X-PLOR Manual Version 3.1*; Yale University: New Haven, CT, 1992. (b) Nilges, M.; Gronenborn, A. M.; Brünger, A. T.; Clore, G. M. *Protein Eng.* **1988**, *2*, 27−38. (c) Brooks, B. R.; Bruccoleri, R. E.; Olafson, B. D.; States, D. J.; Swaminathan, S.; Karplus, M. *J. Comput. Chem.* **1983**, *4*, 187−217.

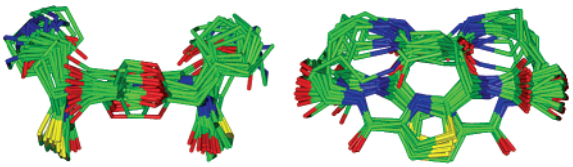

Figure 4. Superimposition of the 20 lowest energy NMR structures of **7** shown end on (left) and side on (right).

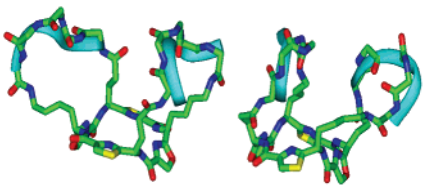

Figure 5. Scaffold from **3** (NMR structure) with two grafted loops (green) excised from crystal structures: (a, left) interhelical regions (A167−171, A230−234) of α-catenin (pdb: 1DOW),[14a] and (b, right) CDR loops L3 (L92−96) and L1 (L24−27) of antibody Igg1 Fab' fragment B13I2 (pdb: 2IGF);[14b] both were modeled using template forcing (Supporting Information) on corresponding 4−5 residue loop fragments (blue ribbons) from crystal structures.[14]

Regioselective formation of oxazole- rather than thiazole-containing loops in **3** may be due to formation of the Glu NH···OC Glu H-bond during loop formation, though we were unable to detect it at low temperatures. Alternatively, steric hindrance from the thiazoles may reduce access of the amine to the bulky activated ester. It is possible that π-complex formation[13] between oxazole and activated ester stabilizes an intermediate for condensation, as suggested by trapping of hydroxybenzotriazole during synthesis.[11]

Isomer **7** was independently synthesized (Scheme 3) from L-Lys(Boc)(Ox)-OMe and Cbz-L-Glu(OtBu)(Thz)-OH instead of **8** and **9**. Like **3**, isomer **7** displayed C_2 fold symmetry in ^{1}H and ^{13}C NMR spectra. NMR parameters for **7** were significantly different from those for **3**, with the Lys αNH resonance (δ 7.95, $^3J_{NH-\alpha H} = 9.32$ Hz) being relatively independent of temperature ($\Delta\delta/T$ 1.0 ppb/K) and likely H-bonded. The Glu αNH and Lys ϵNH resonances are more temperature dependent ($\Delta\delta/T$ 4.0, 3.9 ppb/K, respectively) and also display faster D_2O exchange than Lys αNH. Interestingly, Lys αNH retained its high coupling constant despite the change in loop conformation from over the oxazole to over the thiazole. Like **3**, the loop regions within **7** display significant chemical shift differences for several pairs of geminal protons (Glu-βHs 0.49, Glu-γHs 0.65, Lys-βHs 0.23, and Lys-ϵHs 0.76 ppm), although these differences themselves have changed with respect to **3**.

Due to significant spectral overlap, principally in the Lys $\gamma CH_2/\delta CH_2$ region, NMR structure calculations in XPLOR were based on a smaller subset of 30 distance restraints, together with the Lys dihedral angle and Lys αNH H-bond restraints (Supporting Information). The NMR structures of **7** (Figure 4) indicated that the loops project from one face of the macrocycle but were not as perpendicular as in **3**. The calculated structures for the loops in **7** converged well (loop heavy atom RMSD = 0.9 Å); however, some ROE signals for Lys $\gamma CH_2/\delta CH_2$ could not be assigned. Compared with **3**, the macrocyclic scaffold structures of **7** did not converge as well (backbone RMSD, 0.3 Å), particularly the oxazole rings, which tilt ±20° from the plane of the cyclic scaffold.

Molecular models (Figure 5) suggest that the dimensions and directionality of side chains of the scaffold in **3** match the positions of the interhelical protein loops of helix bundles (Figure 5a) and complementarity-determining loops of antibodies (Figure 5b). The cyclic scaffold **6** in structures **3** and **7** therefore seems appropriate for devising structural mimics of even larger multiloop protein surfaces.

Acknowledgment. We thank Michael Kelso for modifying XPLOR and ARC for some financial support.

Supporting Information Available: Compound syntheses, characterization (NMR, MS, HPLC), computer modeling data, NMR spectra, and structure calculation data for **3** and **7**. This material is available free of charge via the Internet at http://pubs.acs.org.

OL026463M

(13) Hunter, C. A.; Sanders, J. K. M. *J. Am. Chem. Soc.* **1990**, *112*, 5525−5534.

(14) (a) Pokutta, S.; Weis, W. I. *Mol. Cell* **2000**, *5*, 533−43. (b) Stanfield, R. L.; Fieser, T. M.; Lerner, R. A.; Wilson, I. A. *Science* **1990**, *248*, 712−719.